A Simple Approach to Designing and Implementing a Fault Detection Device for Large Quantities of LED Boards

Submitted: 6th April 2025; accepted: 13th May 2025

Van Anh Pham, Minh Tien Do

DOI: 10.14313/jamris-2026-009

Abstract:
Light-emitting diodes (LEDs) play a crucial role in various practical applications. This paper presents a simple and cost-effective approach for detecting faults in LED boards with a large number. The types of faults detected include open circuits and short circuits. The proposed solution is based on a voltage threshold and a statistical algorithm to filter out noise. The paper first outlines the design concept, followed by the development and fabrication of a fault classification module. Subsequently, a control center is established to collect signals from all fault classification modules connected to LED boards in pairs. The received signals are processed and stored on a memory card. Finally, the resulting data can be accessed either from the memory card or directly via an external computer through a USB port. The experimental results demonstrate that the proposed design and fabricated device can accurately detect and classify faults on the tested boards. The data obtained can be used for statistical analysis and root cause investigation to enhance product quality.

Keywords: *LED boards, LFD module, control center, Arduino Mega2560, fault detection model*

1. Introduction

Light-emitting diode (LED) circuit boards are increasingly utilized in lighting, display, and industrial applications due to their high efficiency, long lifespan, and low energy consumption [1–4]. However, during production and operation, LED circuit boards may encounter various faults, such as power supply failures, circuit breaks, semiconductor component damage, or degradation in light quality. Accurate fault detection and diagnosis play a crucial role in maintaining operational performance, reducing repair costs, and extending system longevity.

Some previous studies have focused on fault detection based on image processing techniques combined with an automated optical inspection system [5], achieving an accuracy of up to 95% and a processing speed of 0.3 seconds per image. The study [6] concentrated on the electromechanical characteristics of LEDs that may lead to defects when operating in flammable environments. In [7], the authors employed a backpropagation neural network along with the support vector machine (SVM) algorithm for fault diagnosis. A low-cost method utilizing fault detection on a series of three LEDs was also considered [8], however, this study only addressed automated inspection for a small number of LEDs. Another investigation [9] employed a non-destructive testing method based on a confocal laser scanning microscope system to identify faults under varying inspection durations. A machine learning approach was presented in [10] to predict faults in LEDs. In [11], the authors focused on the frequency-time characteristics of LED light emission to detect faults that conventional measurement methods fail to identify, achieving an accuracy of up to 92% and demonstrating applicability for large-scale LED maintenance. Additionally, a study on detecting short-circuit faults in LEDs based on differences in voltage thresholds by combining a mathematical model with neural networks was mentioned in [12]. Among these methods, most were concentrated on fault detection for a relatively small number of LEDs.

Unlike the aforementioned studies, this paper investigates a fault diagnosis method for LED circuit boards by analyzing abnormal features in the LED shapes on the board and the connecting circuitry. Based on these analyses, an automated fault analysis and detection model is proposed, employing signal processing techniques to enhance the accuracy of identifying the root causes of faults. Our approach is straightforward, cost-effective, and applicable to a large number of LED boards.

This study utilizes electronic measurement techniques and X-ray imaging to construct a fault detection model. Common faults on LED circuit boards such as open circuits, short circuits, and power degradation will be analyzed to determine fault patterns and propose design solutions for fault detection systems.

Moreover, this study identifies the primary causes of failures in LED boards, including individual LEDs, based on an analysis of defect reports received from user partners. The results revealed that damage occurred to the LED components after they were soldered onto an insulated metal substrate (IMS), which served as a heat sink. Figure. 1 illustrates a damaged LED module (coded 2583-164). X-ray images revealed no defects in the electrical circuit on the aluminum heat sink substrate (see Figure. 2). However, the defects were observed in the LED chips. Perpendicular and tilted X-ray images of the LED chip (Figures. 3 and 4) identified anomalies in the defective chips. In contrast, side-view images of the chips did not

Figure 1. A module of 3-LED (SMD 2583-164)

Figure 2. X-ray image of the electrical circuit of the LED board

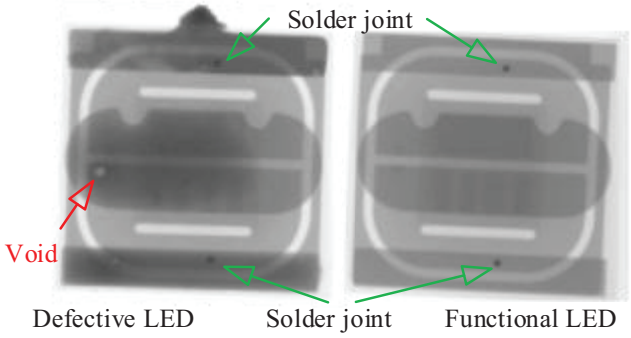

Figure 3. X-ray image showing a defect in the LED chip

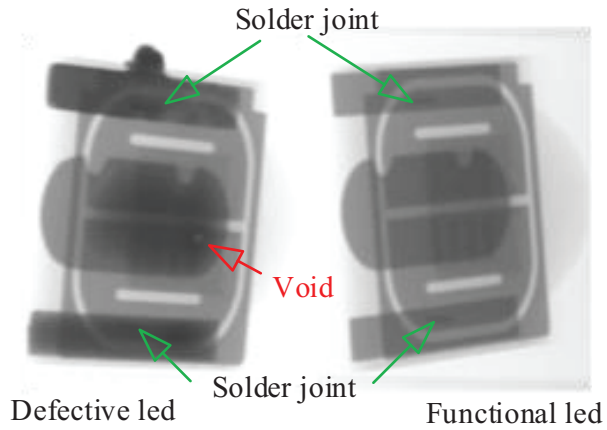

Figure 4. Lateral X-ray image showing a defect on the LED chip

exhibit any distinguishable differences between the functional and defective LEDs, as shown in Figure. 5

In addition to the X-ray method, manual measurements were performed on both functional and faulty LEDs using a digital multimeter (Fluke 87V). An example of the manual measurement results is presented as follows: The light emitted is bright for functional LEDs, with the forward resistance measuring 37.9 MΩ. In contrast, a damaged LED that does not emit light exhibits a resistance value of only 38.2 Ω. The results are illustrated in Figure. 6.

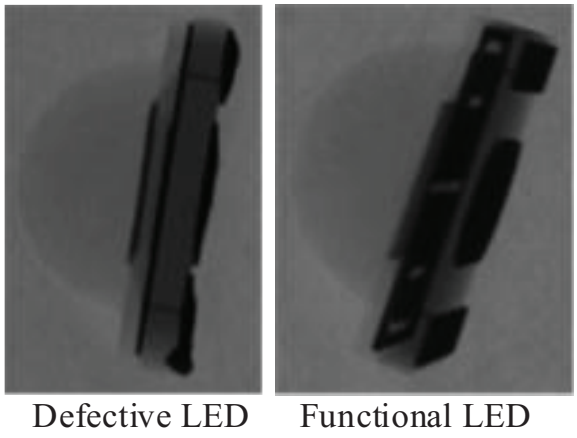

Figure 5. X-ray image of the side view of the defective and functional LEDs

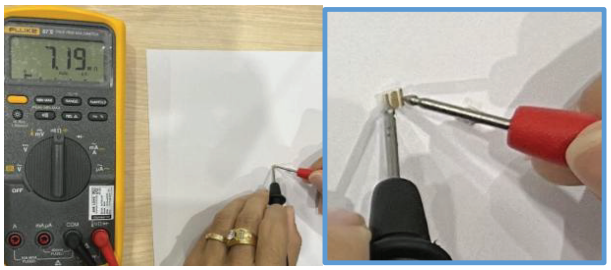

Figure 6. Demonstration of manual resistance measurements for functional and defective LEDs

Based on these observations, the following general design requirements are proposed: a testing duration of 120 minutes, with a cycle consisting of 5 minutes ON and 1 minute OFF. A constant electrical current of 300 to 350 mA that is applied to each 3-LED board, ensuring the current does not exceed 350 mA. The system is capable of automatically detecting short and open circuits in individual LEDs.

This paper proposes an approach for designing testing equipment that simultaneously identifies error types on surface mounted device (SMD) LED boards. The system supports testing of up to 200 3-LED boards or 600 1-LED boards. The device operates based on a voltage threshold to detect open circuits, short circuits, or normal operational statuses of LED boards. The control center, fault collection, and data export are managed by an Arduino Mega2560. This central unit is interfaced with 74HC165 modules to fully expand the data capture ports. The design, manufacturing, and testing processes have demonstrated that the device meets the proposed design requirements and ensures testing accuracy.

The remainder of this paper is organized as follows: Section II presents the conceptual design, Section III details the design of the reporting system, Section IV discusses the experimental fabrication process, and Section V presents the results and their subsequent discussion. Finally, the conclusions are drawn in the last section

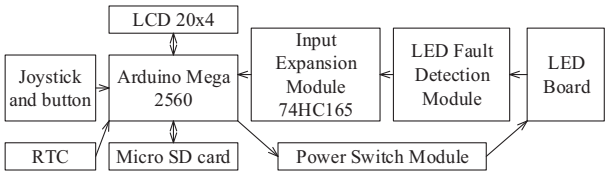

Figure 7. Block schematic of control system

2. Conceptual Design

This section introduces the device's core concept and the essential components for accurate fault diagnostics. A proposed design includes blocks shown in Figure. 7 to implement the requirements check for 200 boards with 3-LED. The control center is an Arduino Mega Kit. This board was selected due to the many digital I/O pins essential for huge LED boards (54 I/O pins). The second important module is the expansion board. One thousand two hundred input pins are necessary to determine the states of 600 LED units. It should be noted that a LED has three states: short, open, and regular circuit. It needs two pins to know the LED state. For the maximum checked LED on each board case, the calculation is conducted with 3-LED boards. Therefore, 150 units of 74HC165 chip can appreciate total LEDs on checked boards.

The following important part is the error classification module. This module outputs three possible statuses for each LED: short, open, and regular circuit. A comparison structure of voltage level can be used to identify the error of a single LED. However, it is necessary to determine the resistance value of false LEDs. Another equally important part is the power supply module. Instead of using relays to turn on or off the LED power supply source, the modules that apply the MOSFET transistor are used to restrict noise that affect feedback signals.

Furthermore, a microSD card is applied to write the result data. This module is directly connected to the center control module. Similarly, an accurate timer is added to write the final time of the testing process. The input commands from the control human are typed to set up the parameter of the testing process through a joystick attached to a switch. This joystick is connected to Arduino Mega through two analog pins and a digital input pin.

3. System Design

3.1. Mechanical Design

Next, a mechanical structure supporting the electric system is designed and presented in Figure. 8. This uses profile aluminum bars 40×40, combined with powder-coated steel sheets as an external cover. Total dimensions are 1100, 1000, and 350 mm, corresponding to height, length, and width. The grooved insulating panels containing the LED boards act as a support floor, separating the floors. Furthermore, an indication lamp is added to identify the device's operation status.

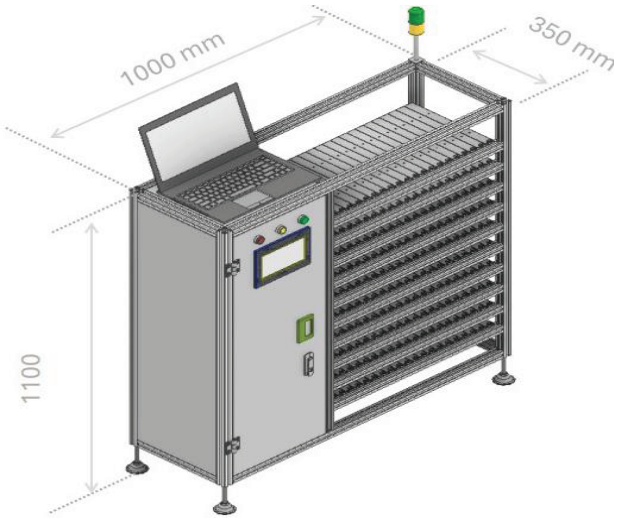

Figure 8. Concept model of mechanical structure

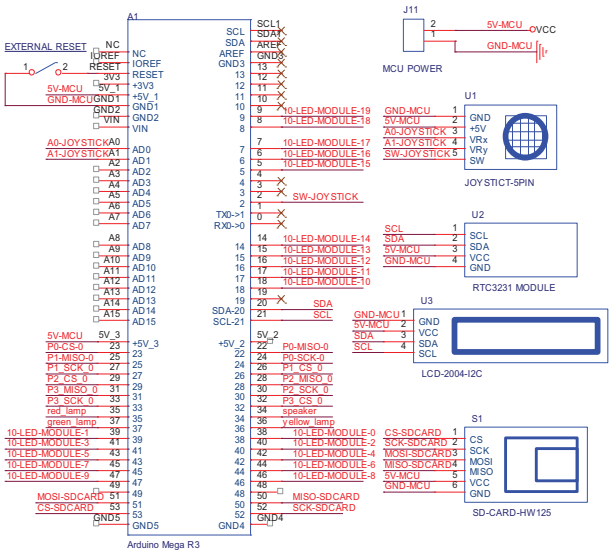

Figure 9. Schematic diagram of control center

3.2. Electrical Design

This section presents the necessary steps of the electronic circuit design process. First, the approach for the control schematics is introduced, as shown in Figure. 9. The control center is optically isolated from the power source of the LED modules and the relays controlling the alarm lamps in order to reduce the impact of signal noise. The modules, including the 3-signal pin joystick, the 20-column × 04-row LCD, the real-time clock (RTC 3231), and the microSD card, are directly connected to the Arduino Mega KIT (see Figure. 9). Two 5V power supply module types are employed: one to power the microcontroller, input expansion modules, LCD, RTC, and SD card, and the other to supply power to the high-power LED modules and fault classification modules. This design ensures the stable operation of the system during extended testing periods.

Additionally, a four-channel relay module is incorporated to operate alarm lamps that indicate the device's operational status. This relay module is

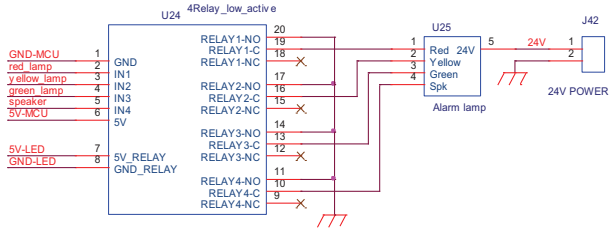

Figure 10. Schematics of the optically isolated relay module

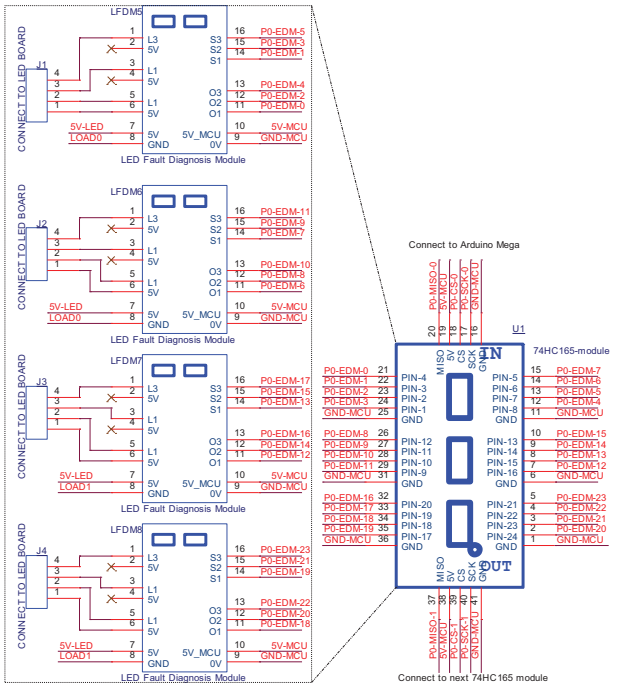

Figure 11. Connection diagram of peripheral devices (74HC165 and LFD module)

optically isolated from the Arduino Mega, as demonstrated in Figure. 10.

The next section of the design diagram illustrates the connection between the LED fault detection (LFD) modules and the input expansion modules based on the 74HC165 shift register. Each LFD module is capable of identifying the failure types of a three-LED board (open, short, and regular circuits). A pin expansion board consists of three 74HC165 chips, providing a total of 24 digital inputs, and is connected to four LFD modules (see Figure. 11). Therefore, for testing 200 LED boards, a total of 600 LFD modules and 50 pin expansion modules are required, which corresponds to 1200 digital data pins transferred to the Arduino Mega KIT.

In this design, due to the reliance on the mechanical frame structure, the port expansion system is distributed across four main blocks, each utilizing three pins: CLK, CS, and MISO, which are connected to the Arduino Mega 2560. The first three blocks contain 13 modules of 74HC165, while the fourth block contains 11 modules

An LFD module consists of three testing clusters, with each cluster monitoring a single LED chip. The

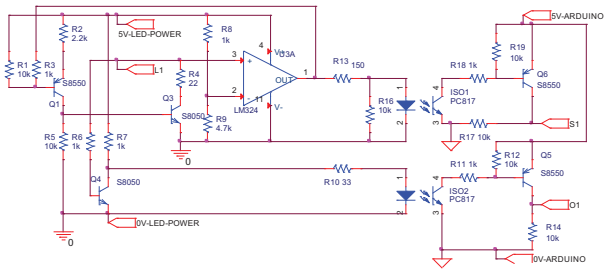

Figure 12. Fault detection circuit of an LED

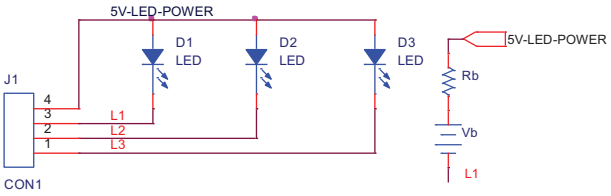

Figure 13. (a) Schematics of a 3-LED module (SMD 2583-164), (b) the DC equivalent circuit of an LED

schematic diagram of the cluster is shown in Figure. 12. It is important to note that an op-amp LM324 is employed to determine whether the LED is experiencing a short circuit or is in normal operation. The classification threshold is set via the voltage divider network comprising resistors *R8* and *R9*. Transistors *Q4*, resistors *R6* and *R7*, are used to detect open-circuit LED faults. The results are communicated through two pins, *O1* and *S1*, which indicate the following statuses: open circuit (if *O1* is high and S1 is low), short circuit (if *S1* is high and *O1* is low), or normal operation (if both *O1* and *S1* are low). The ISO1 and ISO2 optocouplers provide electrical isolation for the test status signal before transmitting the *S1* and *O1* signals to the Arduino Mega KIT. This isolation ensures the stability of the central controller's operation during prolonged testing periods.

The schematic diagram of the LED module to be tested is shown in Figure. 13a. The LEDs are connected to a common anode, with the power pins (*L1*, *L2*, and *L3*) directly connected to the LFD module. The equivalent schematic diagram for a regular, forward-biased LED is presented in Figure. 13b, where the forward voltage $V_F = R_b.I_F + V_b$, with V_b representing the barrier voltage of the LED junction, and *Rb* denoting the internal resistance of the LED.

3.3. Control Flow Chart

The primary control algorithm, as illustrated in Figure. 14, provides a clearer understanding of the device's operation. There are three main operating modes: Setup Mode (i), Calibration Mode (ii), and Testing Mode (iii). In Mode (i), users can configure input parameters such as the number of boards to be tested, the LED "on" time (t_{on}), the LED "off" time (t_{off}), and the total testing time (t_c). It should be noted that the number of LED testing cycles (n_c) is calculated as follows: n_c = ROUNDDOWN(t_c / (t_{on} + t_{off})), where ROUNDDOWN(.) denotes the floor function. In Mode

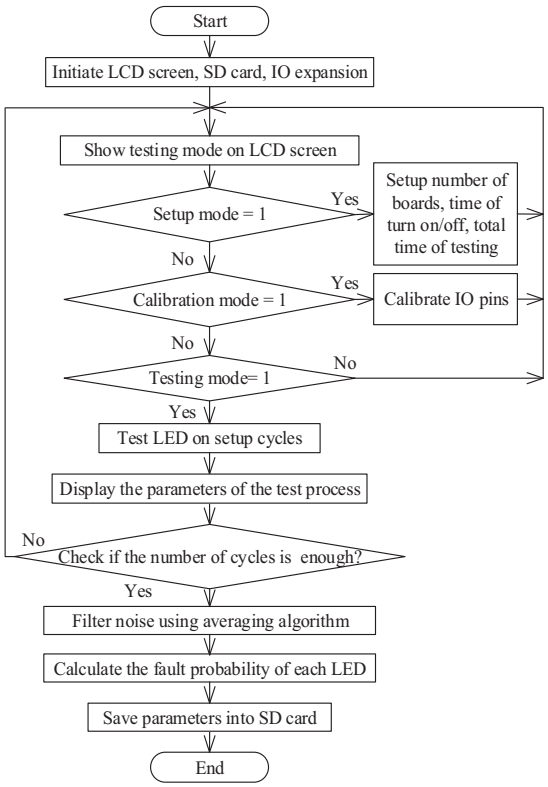

Figure 14. Schematics of control flowchart

(ii), users can perform diagnostics on the extended I/O ports without connecting to the LED modules. This mode enables the verification of the status of the extended ports and the identification of potential faults in the associated internal modules. Mode (iii) is the testing operation to determine whether LEDs are faulty or operational when connected to the device. In this mode, the LED modules are switched on and off cyclically. During the "on" state, the fault detection signal is sampled continuously at a frequency of 1 Hz throughout the "on" period (ton), which minimizes the impact of signal noise during testing. A parameter, referred to as the actual fault return frequency (f_{Ei}), is introduced and calculated as follows: $f_{Ei} = n_{Ei}/n_T$, where n_{Ei} is the number of detected faults, n_T denotes the total number of sampling acquisitions during the testing process, and $i = 1, 2, ..., 1200$. It should be noted that n_{Ei} is computed as follows:$n_{Ei} = \sum_{j=1}^{n_T} x_{Ki}\,[j]$, where, x_{Ki} represents the logic value of the output K at position i, if i is an even number, then $K = O$ else $K = S$; O and S are symbols related to the output state pin of the LFD board. The parameter f_{Ei} is crucial for evaluating the reliability of the testing process, especially in industrial environments. A fault is confirmed to have occurred when $f_{Ei} \geq f_T$, $f_T$is the threshold value. Beyond averaging-based noise filtering, sequential switching of 20 LR7843 power modules is employed to minimize system interference.

In summary, integrating noise filtering algorithms, rational power switching control, and microcontroller–power stage isolation enhances system stability and reliability.

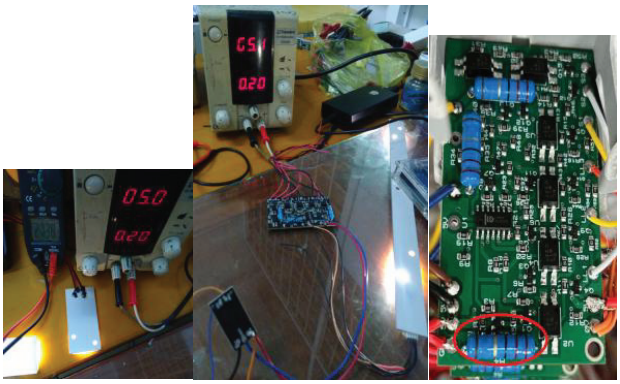

Figure 15. Illustration of the measurement of current and voltage parameters on 1-Led model: SMD 2583-426 REV B (a), 3LED board model: SMD 2583-164 PCB REV B (b), and fault classification module (c)

4. Manufacturing process

The fabrication process of the device consists of two primary stages: the experimental phase (i) and the manufacturing phase (ii). In the first stage (i), the fault classification module for a single LED unit is tested. This process involves conducting manual measurements to identify fault types and testing a prototype of the fault classification module, which is connected to a 3-LED board using a multimeter and a digital power supply (Topward 3303D). This procedure is illustrated in Figure. 15. It is important to note that the SMD 2583-426 LED module contains a single LED, whereas the SMD 2583-164 module contains three LEDs. These modules are not equipped with current-limiting resistors (refer to Figure. 13). The second stage (ii) entails the mass production of LFD modules and their integration with extended I/O modules, Mosfet LR7843-based PWM controller modules (HW-532), and the central controller (Arduino Mega 2560). The LED boards to be tested are systematically arranged across eight levels of a storage cabinet, with each level accommodating 25 LED boards. Each HW-532 module is employed to power 10 to 12 LFD modules. This module was selected due to its resistance characteristics, with $R_{DS(on)max}$ = *3.3 mΩ*, leading to a voltage drop across the power module is low, $V_{DS(on)}$ = $R_{DS(on)max} \times I_{max} \approx 0.043\ V$. Four 5VDC, 20A power supplies are evenly distributed to supply power to the eight levels of LED boards (200 3LED-boards) and the 200 LFD boards. The power supply, with $V_p = 5V$, was selected due to its widespread industrial adoption and compatibility with the forward voltage of the LED chip. The current per three-LED board, $I_{3LB\,\max}$, is limited to 350 mA. Consequently, the maximum average current per LED is given by $I_{F\,\max} = I_{3LB\,\max}/3$. The total peak power of the device, $P_{D\,\max} = 600 I_{F\,\max} V_P = 350W$, remains within safe operational limits. Although the chosen 400W total power is not fully optimized, it ensures a reliable safety margin for the system.

Figure 16. LED fault tester during assembly and testing

To demonstrate the results of the manufacturing process, Figures. 16 and 17 illustrate the assembly of modules into the mechanical cabinet, along with the testing of each part before the final device inspection. Additionally, this process includes the calibration of I/O expansion modules to fix any errors.

5. Results and Discussion

To further evaluate the device before completion, we tested some samples sent by customers. The number of sample boards used for testing the device is 5 (for 3-led boards), named NCR1 to NCR5 and illustrated in Figure. 18. First, these sample LED boards manually tested each LED by using the multimeter for resistor measurement and the digital power supply to track consumed current, to determine the fault types. Then, they are connected to only one individual LFD module and the digital power source to confirm. This process is to claim that the faulty kind of sample boards are exact. Results are summarized in Table 1. It is noted that the returned output values of the LFD module are shown in this table, where Oi and Si indicate "open state" and "short state" correspondingly ($i = 1, 2, 3$). Next, five sample boards are attached to the manufactured testing device, and the position of the connector jacks is marked. The device is activated, and the testing results are compared to the sample set. Figure. 19 illustrates the diagram of the testing process. The test results are performed 40 times with a shortened time of 2 minutes ON time and 1 minute OFF time. This test is because the number of boards with broken LEDs is limited. The test time is shortened compared to reality, but the number of tests performed has increased (up to 40 times). The positions not connected to the LED boards are considered open circuit fault board one during the test.

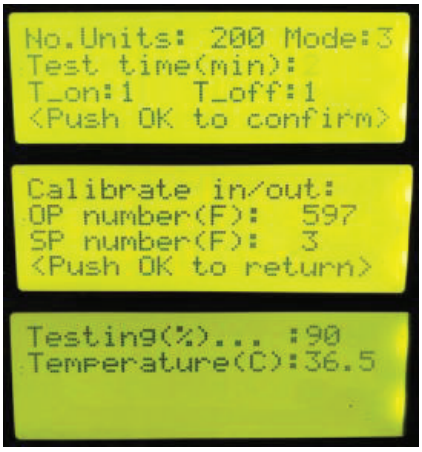

Figure 17. Display screen of parameters

Figure 18. Testing board samples (2583-164-PCB-REV B, 2583-426-REV B)

The results of the individual tests are presented in Figure. 20. The key parameters include the test date and time, the circuit board position, the LED location, the test status, and the probability of meeting the required criteria. It is important to note that the probability of meeting the criteria is calculated as the ratio of successful trials to the total number of tests conducted. This value corresponds to f_{Ei} as mentioned in Section 3.3. The test status is determined during the period when the LED is illuminated. Due to measurement noise, this parameter may not reach a value of 1, but it reflects the reliability of the test results. Experimental results demonstrate that the device's trial runs accurately identified errors on the sample LED boards, including LED location, board position, and fault type. A total of 40 tests were performed, all of which met the required criteria.

To further assess the accuracy and reliability of the device, a statistical analysis was conducted with 40 different trials using five 3-LED board samples per run at varying positions, i.e., the evaluation used 15 LEDs, including 3 open-circuit, 2 short-circuit, and 10 functioning LEDs (see Table 1) for each trial. This arrangement ensures that all 600 positions were tested once. The device accurately identified the correct status of each LED in all trials. Therefore, the observed accuracy is 100%. Using the Wilson score interval method, the 95% confidence interval for the true accuracy of the device was estimated to be no less than 99.37%. These results indicate that the device is highly reliable.

In addition to the inspection status of the LEDs derived from the data stored on the SD card, the device

Table 1. Sample of faulty LED boards (2583-164-PCB-REV B).

	N.o. Board	NCR1	NCR2	NCR3	NCR4	NCR5
LED1	Led1 State	O	N	N	N	N
	O pin	1	0	0	0	0
	S pin	0	0	0	0	0
LED2	Led2 State	N	N	S	O	S
	O pin	0	0	0	1	0
	S pin	0	0	1	0	1
LED3	Led3 State	N	O	N	N	N
	O pin	0	1	0	0	0
	S pin	0	0	0	0	0

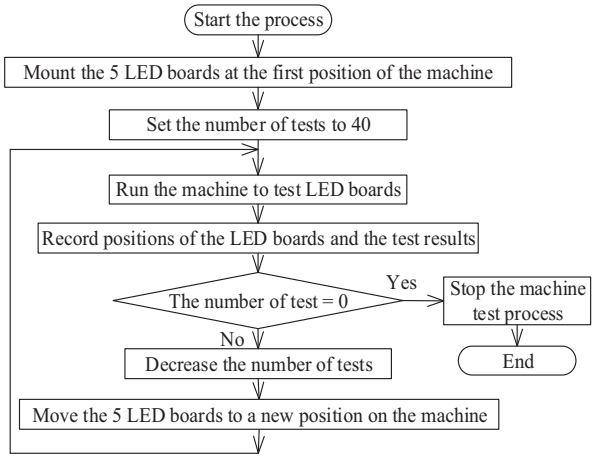

Figure 19. Illustration of the device testing process with a small number of faulty LED boards

474	Number of LED unit s: 200					
475	Total time of test ing (minutes): 2					
476	Time of on Led (minutes): 1					
477	Time of off Led (minutes): 1					
478	Date	Time	No.board	No.led	Status	Probability
479	8/9/2024	16:50	1	1	Open	1
480	8/9/2024	16:50	2	3	Open	1
481	8/9/2024	16:50	3	2	Short	1
482	8/9/2024	16:50	4	2	Open	1
483	8/9/2024	16:50	5	2	Short	1
484	8/9/2024	16:50	6	1	Open	1
485	8/9/2024	16:50	6	2	Open	1
486	8/9/2024	16:50	6	3	Open	1
487	8/9/2024	16:50	7	1	Open	1
488	8/9/2024	16:50	7	2	Open	1
489	8/9/2024	16:50	7	3	Open	1
490	8/9/2024	16:50	8	1	Open	1
491	8/9/2024	16:50	8	2	Open	1
492	8/9/2024	16:50	8	3	Open	1
493	8/9/2024	16:50	9	1	Open	1
494	8/9/2024	16:50	9	2	Open	1
495	8/9/2024	16:50	9	3	Open	1
496	8/9/2024	16:50	10	1	Open	1
497	8/9/2024	16:50	10	2	Open	1
498	8/9/2024	16:50	10	3	Open	1

Figure 20. A report sample of the testing result

was also tested for current and voltage values directly across the LEDs using a manual random measurement method with a multimeter. The results are as follows: the average current through each LED ranged from 96 mA to 100 mA, and the forward voltage ranged from 2.7 V to 3.0 V. These values conform to the required specifications. A slight deviation between the calculated and measured values was observed, attributable to the cable resistance connecting the LED boards and LFD modules. The average actual power consumption of a functional LED is calculated as $P_1 = \bar{I}_F \bar{V}_F \approx 0.28\ W$, while the average power consumption of an LED branch and the testing circuit is $P_2 = \bar{I}_F V_P \approx 0.49\ W$, where the average current through a single LED is $\bar{I}_F = 0.098\ A$ and the average voltage drop across the LED is $\bar{V}_F = 2.85\ V$. Consequently, the calculated energy efficiency of the testing device is $\eta = P_1/P_2 = 0.57$, which remains suboptimal. To enhance efficiency, future design adjustments may be necessary, particularly by lowering the supply voltage.

In comparison with previous research methods that employed image processing techniques [5], neural networks combined with SVM [7], and learning machines [10], which achieved high accuracy for small-scale inspections but incurred high computational costs, our presented approach is simpler and computationally efficient on low-end processors. Moreover, it can be easily calibrated and scaled for high-throughput inspection.

In summary, the device trial met the essential requirements, effectively distinguishing the states of the LED boards. However, the practical testing process revealed some limitations: the sample size was insufficient, with only five boards tested across 40 trials; the device was tested solely on 3-LED boards, without comprehensive testing on 1- or 2-LED boards.

Additionally, long-cycle sequential testing was not performed due to the significant time required. One reason for this limitation was the insufficient number of 1-LED and 2-LED boards provided by the customer. Nonetheless, the 1-LED and 2-LED boards share the same LED components as the 3-LED boards and lack current-limiting resistors (see Figure 13a). Therefore, the 3-LED boards were considered representative and used as substitutes for the other types during testing. Finally, the device has been transferred to the operational unit without reported issues, except for a request to update the control program to enable the display of inspection data for LED boards. The Arduino

program source code is accessible at: https://github.com/anhcdt/ArduinoMega-code/tree/main

6. Conclusion

In this paper, a design proposal and implementation of a testing device for detecting LED failures on circuit boards have been carried out. The design solution is based on classifying the operating conditions of each LED: open circuit, short circuit, and regular. The classification circuit relies on the working resistance threshold of the LED to identify faults. To enable simultaneous testing of multiple circuit boards, the central control circuit utilizes an Arduino Mega and 74HC165 input expansion modules, allowing for an extension of up to 1200 inputs. The control algorithm operates based on calculating continuous sampling frequency throughout the operating period to accurately determine the status of each LED and generate the result report, which can be accessed directly via a USB-Comport connection or indirectly via a memory card. The test results indicate that the designed device can accurately detect the faults present in LED boards. In the future, several works can be identified as follows:

(i) A comprehensive and diverse set of circuit board samples from the factory will be collected for testing and overall machine evaluation in a continuous improvement cycle.

(ii) A machine learning-based approach will be incorporated to analyze fault patterns using time-series data storage, particularly in design enhancements for expanding RGB LEDs, high-power COB LEDs, or multi-channel LED systems.

(iii) The system will be connected to Internet of Thing (IoT) platforms via Bluetooth and Wi-Fi, enabling real-time remote monitoring and predictive maintenance.

(iv) A GUI-based interface will be developed to display results within an industrial setting.

(v) Optimization of the device's energy efficiency will also be considered in machine design adjustments.

AUTHORS

Van Anh Pham* – Department of Mechatronics, Faculty of Technology Engineering, Pham Van Dong University, Cam Thanh ward, 53129, Quang Ngai province, Vietnam, e-mail: pvanh@pdu.edu.vn, https://orcid.org/0000-0002-6793-5260.

Minh Tien Do – Department of Mechanical Engineering, Faculty of Technology Engineering, Pham Van Dong University, Cam Thanh ward, 53129, Quang Ngai province, Vietnam, e-mail: dmtien@pdu.edu.vn.

*Corresponding author

ACKNOWLEDGEMENTS

We would like to thank the engineer, Cat Len Le, from DKMEC Company for designing the chassis frame and providing valuable design input for this project.

References

[1] X. Long et al., "A Review on Light-Emitting Diode Based Automotive Headlamps," *Renewable and Sustainable Energy Reviews*, vol. 41, 2015, pp. 29–41.

[2] D. Busek and K. Dusek, "Overview of Various Failures of Luminaires Assembled with SMD LED Chips," *2022 45th International Spring Seminar on Electronics Technology (ISSE)*, 2022, pp. 1–5.

[3] M. Esteki et al., "LED Systems Applications and LED Driver Topologies: A Review," *IEEE Access*, vol. 11, 2023, pp. 38324–38358.

[4] R. Sananda, C. Tejaswi, and B. Rishaya, "Trends and Challenges in Automotive Headlamps," *Proc.SPIE*, vol. 12638, 2023, p. 126380R.

[5] D.-B. Perng, H.-W. Liu, and C.-C. Chang, "Automated SMD LED Inspection using Machine Vision," *The International Journal of Advanced Manufacturing Technology*, vol. 57, no. 9, 2011, pp. 1065–1077.

[6] K. Fumagalli, R. Faranda, and L. Farnè, "Analysis of Possible LED Failure Mode," *2014 Petroleum and Chemical Industry Conference Europe*, 2014, pp. 1–8.

[7] H. Jiang et al., "LED Device Fault Diagnosis Base on Neural Network and SVM Model Analysis," *2017 14th China International Forum on Solid State Lighting: International Forum on Wide Bandgap Semiconductors China (SSLChina: IFWS)*, 2017, pp. 45–47.

[8] A. Arora and V. Goel, "Real Time Fault Analysis and Acknowledgement System for LED String," *2018 International Conference on Computing, Power and Communication Technologies (GUCON)*, 2018, pp. 457–461.

[9] H. K. Fu et al., "Accelerated Life Testing and Fault Analysis of High-Power LED," *IEEE Transactions on Electron Devices*, vol. 65, no. 3, 2018, pp. 1036–1042.

[10] M. S. Ibrahim et al., "Machine Learning and Digital Twin Driven Diagnostics and Prognostics of Light-Emitting Diodes," *Laser & Photonics Reviews*, vol. 14, no. 12, 2020, p. 2000254.

[11] Y. Shang et al., "A Novel Fault Diagnosis Strategy for LED Lamps via Light Output Time-Frequency Characteristics Analysis and Machine Learning," *Heliyon*, vol. 9, no. 9, 2023.

[12] J. R. Martínez-Pérez et al., "Advanced Detection of Failed LEDs in a Short Circuit for Automotive Lighting Applications," *Sensors*, vol. 24, no. 9; doi: 10.3390/s24092802.